Modified MacAyeal-Morland Model

Aitbala Sargent, James Fastook

Climate Change Institute
University of Maine, Orono, ME

October 8-10, 2008
West Antarctic Ice Sheet Initiative

Table of contents

Ice stream modeling

Modified MacAyeal-Morland model

Model Verification

Summary

Table of contents

Ice stream modeling

Modified MacAyeal-Morland model

Model Verification

Summary

Ice streams

- lightly grounded;
- low driving stresses;
- high speed: 300 - 900 m/year.

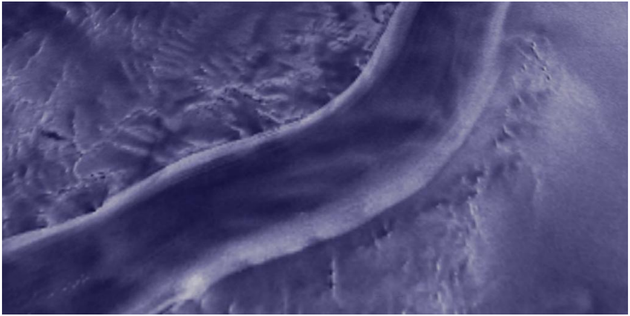

Figure: *NASA/Goddard Space Flight Center - Scientific Visualization Studio Canadian Space Agency RADARSAT International Inc.*

Ice stream modeling

3-Dimensional models

$$
\begin{aligned}
\frac{\partial \sigma_{xx}}{\partial x} + \frac{\partial \sigma_{xy}}{\partial y} + \frac{\partial \sigma_{xz}}{\partial z} &= \rho g_x\,, \\
\frac{\partial \sigma_{yx}}{\partial x} + \frac{\partial \sigma_{yy}}{\partial y} + \frac{\partial \sigma_{yz}}{\partial z} &= \rho g_y\,, \\
\frac{\partial \sigma_{zx}}{\partial x} + \frac{\partial \sigma_{zy}}{\partial y} + \frac{\partial \sigma_{zz}}{\partial z} &= \rho g_z\,.
\end{aligned}
$$

- all stresses are included;
- computationally time demanding.

Ice stream modeling

MacAyeal-Morland model

- ice-shelves: basal stresses neglected (Z is integrated out $\rightarrow$ 2-D)

$$\frac{\partial}{\partial x}\left[2\bar{\mu}h(2\dot{\epsilon}_{xx}+\dot{\epsilon}_{yy})\right]+\frac{\partial}{\partial y}(2\bar{\mu}h\dot{\epsilon}_{xy})=\rho gh\frac{\partial z_s}{\partial x},$$
$$\frac{\partial}{\partial x}(2\bar{\mu}h\dot{\epsilon}_{yx})+\frac{\partial}{\partial y}\left[2\bar{\mu}h(\dot{\epsilon}_{xx}+2\dot{\epsilon}_{yy})\right]=\rho gh\frac{\partial z_s}{\partial y}$$

- ice-streams: the basal drag is added into the equations

$$RHS_x=\rho gh\frac{\partial z_s}{\partial x}+\tau_c\frac{u_x}{|\vec{u}|},RHS_y=\rho gh\frac{\partial z_s}{\partial y}+\tau_c\frac{u_y}{|\vec{u}|}$$

Goal - include the basal drag in the derivation of the equations.

Table of contents

Ice stream modeling

Modified MacAyeal-Morland model

Model Verification

Summary

Mass-balance

Map-plane mass-balance equation

$$\frac{\partial h}{\partial t} = \dot{a} - \frac{\partial q_x}{\partial x} - \frac{\partial q_y}{\partial y}, \text{ where } q_x = U_x h, q_y = U_y h$$

h	thickness	q_x, q_y	flux components
$\dot{a}$	accum. rate	U_x, U_y	vert.-aver. vel. components

Conservation of energy (temperature) equation

$$\frac{\partial T}{\partial t} + \vec{U} \cdot \nabla T + w \frac{\partial T}{\partial z} = K \frac{\partial^2 T}{\partial z^2} + \text{strain-heating}$$

T	ice temperature	$\vec{U}$	vert.-aver. hor. velocity
K	conductivity of ice	w	vertical velocity

Glen's flow law

Stress in terms of strain rate

$$\sigma\prime_{ij} = 2\mu(\dot{\epsilon}, T^*)\dot{\epsilon}_{ij}$$

Effective viscosity

$$\mu = \frac{1}{2}B\dot{\epsilon}^{\frac{1-n}{n}}$$

$\sigma\prime_{ij}$	stress deviator tensor	B	ice hardness
$\dot{\epsilon}_{ij}$	strain rate tensor	n	stress exponent
$\dot{\epsilon}$	second invariant of $\dot{\epsilon}_{ij}$	T^*	homologous temperature

Conservation of momentum

conservation of momentum

$$\frac{\partial \sigma_{xx}}{\partial x} + \frac{\partial \sigma_{xy}}{\partial y} + \frac{\partial \sigma_{xz}}{\partial z} = \rho g_x,$$
$$\frac{\partial \sigma_{yx}}{\partial x} + \frac{\partial \sigma_{yy}}{\partial y} + \frac{\partial \sigma_{yz}}{\partial z} = \rho g_y,$$
$$\frac{\partial \sigma_{zx}}{\partial x} + \frac{\partial \sigma_{zy}}{\partial y} + \frac{\partial \sigma_{zz}}{\partial z} = \rho g_z.$$

which can be written in compact form as

$$\frac{\partial \bar{\sigma}_{ij}}{\partial x_j} - \rho g \delta_{i3} = 0, \text{ where}$$

$$\bar{\sigma} = \begin{bmatrix} \sigma_{xx} & \sigma_{xy} & \sigma_{xz} \\ \sigma_{xy} & \sigma_{yy} & \sigma_{yz} \\ \sigma_{xz} & \sigma_{yz} & \sigma_{zz} \end{bmatrix}.$$

Boundary conditions on surface and base

traction on any surface has components:

$$t_i = \bar{\sigma}_{ij} n_j, \; (i = x, y, z)$$

where $\vec{n} = (n_1, n_2, n_3)$ is unit outward normal.

Boundary conditions on surface and base

on the surface $z = z_s(x, y)$, which is traction free,

$$\bar{\sigma}_{ij} n_j = 0, \text{ where}$$

$$(n_1, n_2, n_3) = \left\{ 1 + \left(\frac{\partial z_s}{\partial x} \right)^2 + \left(\frac{\partial z_s}{\partial y} \right)^2 \right\}^{-\frac{1}{2}} \left[-\frac{\partial z_s}{\partial x}, -\frac{\partial z_s}{\partial y}, 1 \right]$$

on the base $z = z_b(x, y)$, traction is specified as

$$\bar{\sigma}_{ij} n_j = \vec{g} n_i, \text{ where}$$

$$(n_1, n_2, n_3) = \left\{ 1 + \left(\frac{\partial z_b}{\partial x} \right)^2 + \left(\frac{\partial z_b}{\partial y} \right)^2 \right\}^{-\frac{1}{2}} \left[\frac{\partial z_b}{\partial x}, \frac{\partial z_b}{\partial y}, -1 \right],$$

and $\vec{g}$ is a traction in the local system of coordinates perpendicular to $\vec{n}$ and $\vec{y}$ and $\vec{n}$ and $\vec{x}$.

Local normal and tangential to surface or bed coordinate system $\{\vec{m_x}, \vec{m_y}, \vec{n}\}$

$$\vec{m_x} = (\vec{y} \times \vec{n}) = \begin{vmatrix} i & j & k \\ 0 & 1 & 0 \\ n_1 & n_2 & n_3 \end{vmatrix}$$

$$= (n_3, 0, -n_1),$$

$$\vec{m_y} = (\vec{n} \times \vec{x}) = \begin{vmatrix} i & j & k \\ n_1 & n_2 & n_3 \\ 1 & 0 & 0 \end{vmatrix}$$

$$= (0, n_3, -n_2)$$

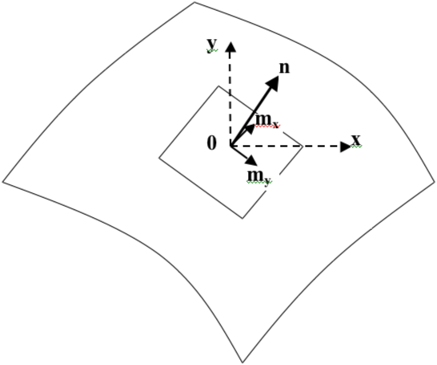

Figure: Local normal and tangential to surface or bed coordinate system

Boundary conditions on the surface and the base

Tangential traction in the coordinate system $\{\vec{m}_x, \vec{m}_y, \vec{n}\}$:

$$\tau_x = \vec{n}\bar{\sigma}\vec{mi}_x = (n_1, n_2, n_3) \begin{vmatrix} \sigma_{xx} & \sigma_{xy} & \sigma_{xz} \\ \sigma_{yx} & \sigma_{yy} & \sigma_{yz} \\ \sigma_{zx} & \sigma_{zy} & \sigma_{zz} \end{vmatrix} \begin{pmatrix} n_3 \\ 0 \\ -n_1 \end{pmatrix}$$

$$= n_1 n_3(\sigma_{xx} - \sigma_{zz}) + n_2 n_3 \sigma_{xy} + (n_3^2 - n_1^2)\sigma_{xz} - n_1 n_2 \sigma_{yz}.$$

$$\tau_y = \vec{n}\bar{\sigma}\vec{mi}_y = (n_1, n_2, n_3) \begin{vmatrix} \sigma_{xx} & \sigma_{xy} & \sigma_{xz} \\ \sigma_{yx} & \sigma_{yy} & \sigma_{yz} \\ \sigma_{zx} & \sigma_{zy} & \sigma_{zz} \end{vmatrix} \begin{pmatrix} 0 \\ n_3 \\ -n_2 \end{pmatrix}$$

$$= n_2 n_3(\sigma_{yy} - \sigma_{zz}) + n_1 n_3 \sigma_{xy} + (n_3^2 - n_2^2)\sigma_{yz} - n_1 n_2 \sigma_{xz}.$$

Boundary conditions on the surface: $\tau_x = 0, \tau_y = 0.$

Boundary conditions on the base: $\tau_x = g_x, \tau_y = g_y,$

where g_x and g_y are defined in the next slide.

Basal Stresses in coordinate system $(\vec{x}, \vec{y}, \vec{z})$

Assumptions in the

MacAyeal-Morland Model: $\vec{f} = (0, 0, \rho g h)$

Modified Model 1: $\vec{f} = \left(-\tau_x \frac{u_x}{|\vec{u}|}, -\tau_y \frac{u_y}{|\vec{u}|}, \rho g h\right)$

Modified Model 2: $\vec{f} = \left(\alpha_x \rho g h \frac{\partial z_s}{\partial x}, \alpha_y \rho g h \frac{\partial z_s}{\partial y}, \rho g h\right)$

where τ_x, τ_y approximate till yield stresses,

$$\text{and } \alpha_x, \alpha_y = \begin{cases} 1 & \text{for ice-sheets,} \\ (0,1) & \text{for ice-streams,} \\ 0 & \text{for ice-shelves.} \end{cases}$$

Basal Stresses in coordinate system $(\vec{m}_x, \vec{m}_y, \vec{n})$

Transformation formulas

$$g_x = \frac{(\vec{f} \cdot \vec{m}_x)}{|\vec{m}_x|} = \frac{f_x n_3 + f_y 0 + f_z(-n_1)}{\sqrt{n_3^2 + 0^2 + (-n_1)^2}}$$

$$= -\left[f_x + f_z \frac{\partial z_b}{\partial x}\right] \left\{1 + \left(\frac{\partial z_b}{\partial x}\right)^2\right\}^{-\frac{1}{2}},$$

$$g_y = \frac{(\vec{f} \cdot \vec{m}_y)}{|\vec{m}_y|} = \frac{f_x 0 + f_y n_3 + f_z(-n_2)}{\sqrt{0^2 + n_3^2 + (-n_2)^2}}$$

$$= -\left[f_y + f_z \frac{\partial z_b}{\partial y}\right] \left\{1 + \left(\frac{\partial z_b}{\partial y}\right)^2\right\}^{-\frac{1}{2}}$$

Basal Stresses in coordinate system $(\vec{m}_x, \vec{m}_y, \vec{n})$

Modified Model 1

$$g_x = -\left[\rho g h \frac{\partial z_b}{\partial x} - \tau_x \frac{u_x}{|\vec{u}|}\right] \left\{1 + \left(\frac{\partial z_b}{\partial x}\right)^2\right\}^{-\frac{1}{2}},$$

$$g_x = -\left[\rho g h \frac{\partial z_b}{\partial y} - \tau_y \frac{u_y}{|\vec{u}|}\right] \left\{1 + \left(\frac{\partial z_b}{\partial y}\right)^2\right\}^{-\frac{1}{2}}$$

Modified Model 2

$$g_x = -\rho g h \left[\frac{\partial z_b}{\partial x} + \alpha_x \frac{\partial z_s}{\partial x}\right] \left\{1 + \left(\frac{\partial z_b}{\partial x}\right)^2\right\}^{-\frac{1}{2}},$$

$$g_y = -\rho g h \left[\frac{\partial z_b}{\partial y} + \alpha_y \frac{\partial z_s}{\partial y}\right] \left\{1 + \left(\frac{\partial z_b}{\partial y}\right)^2\right\}^{-\frac{1}{2}}$$

Assumptions necessary to obtain "reduced" MacAyeal-Morland model

Horizontal velocities and strain rates are uniform in depth:

$$\frac{\partial \dot{\epsilon}_{xx}}{\partial z} \to 0, \quad \frac{\partial \dot{\epsilon}_{yy}}{\partial z} \to 0, \quad \frac{\partial \dot{\epsilon}_{xy}}{\partial z} \to 0,$$
$$\frac{\partial u_x}{\partial z} \to 0, \quad \frac{\partial u_y}{\partial z} \to 0, \quad \dot{\epsilon}_{zx} = \dot{\epsilon}_{zy} = 0.$$

- For ice shelves, these assumptions are justified by their flat and thin geometry;
- MacAyeal-Morland model for ice-streams uses these assumptions for ice-streams as well.

Modified MacAyeal-Morland model

Integration of the horizontal balance equation through the ice thickness $[z_b, z_s]$, together with surface and base boundary conditions, yields:

$$\frac{\partial}{\partial x}\left[2\bar{\mu}h(2\dot{\epsilon}_{xx}+\dot{\epsilon}_{yy})\right]+\frac{\partial}{\partial y}(2\bar{\mu}h\dot{\epsilon}_{xy})=RHS,$$

where *RHS* is as follows in

MacAyeal-Morland Model for ice-shelves:	$\rho g h \frac{\partial z_s}{\partial x}$
MacAyeal-Morland Model for ice-streams:	$\rho g h \frac{\partial z_s}{\partial x} + \tau_c \frac{u_x}{\lvert\vec{u}\rvert}$
Modified Model 1:	$\rho g h \frac{\partial z_s}{\partial x} + \left(\tau_x \frac{u_x}{\lvert\vec{u}\rvert} - \rho g h \frac{\partial z_b}{\partial x}\right) g_{bx}$
Modified Model 2:	$\rho g h \frac{\partial z_s}{\partial x} - \rho g h \left(\alpha_x \frac{\partial z_s}{\partial x} + \frac{\partial z_b}{\partial x}\right) g_{bx}$

where $g_{bx} = \left(1 + (\frac{\partial z_b}{\partial x})^2 + (\frac{\partial z_b}{\partial y})^2\right)\left(1 + \left(\frac{\partial z_b}{\partial x}\right)^2\right)^{-\frac{1}{2}}$

Modified equations take into account the bed profile.

Modified MacAyeal-Morland model for flat bed

$$\frac{\partial}{\partial x}\left[2\bar{\mu}h(2\dot{\epsilon}_{xx}+\dot{\epsilon}_{yy})\right]+\frac{\partial}{\partial y}(2\bar{\mu}h\dot{\epsilon}_{xy})=RHS,$$

where *RHS* is as follows in

MacAyeal-Morland Model for ice-shelves:	$\rho g h \frac{\partial z_s}{\partial x}$
MacAyeal-Morland Model for ice-streams:	$\rho g h \frac{\partial z_s}{\partial x} + \tau_c \frac{u_x}{\lvert\vec{u}\rvert}$
Modified Model 1:	$\rho g h \frac{\partial z_s}{\partial x} + \tau_x \frac{u_x}{\lvert\vec{u}\rvert}$
Modified Model 2:	$\rho g h \frac{\partial z_s}{\partial x} - \rho g h \alpha_x \frac{\partial z_s}{\partial x}$

Table of contents

Ice stream modeling

Modified MacAyeal-Morland model

Model Verification

Summary

Verification of the Modified MacAyeal-Morland model

To verify the model, we simulated the following problems:

- EISMINT 1 test: flow of an ice-shelf into which an ice-stream discharges. Results are compared with MacAyeal (1994).
- 2-D simulation of a subglacial lake with Model 2:
$$\alpha_x = \alpha_y = \begin{cases} 0 & \text{over an artificial lake,} \\ 1 & \text{everywhere else.} \end{cases}$$
- 2-D simulation of ice flow in a rectangular sheet-stream-shelf embayment with Model 2:
$$\alpha_x = \begin{cases} 1 & \text{in the ice-sheet area,} \\ (0, 1) & \text{in the ice-stream area,} \\ 0 & \text{in the ice-shelf area.} \end{cases}$$

EISMINT 1 test: Initial and Boundary Conditions and Finite Element Mesh

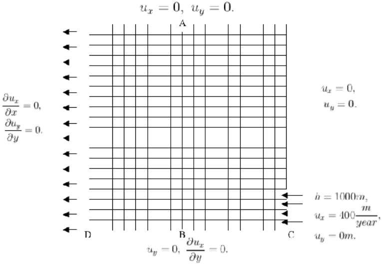

Figure: Finite Element Mesh and Boundary Conditions. Mesh: 17x21 nodes, mesh resolution corresponds to 5 km. Boundary conditions: the kinematic boundary condition associated with ice-stream input is specified on the bottom 4 nodes of the right boundary; The ice front corresponds to the right boundary; The lower boundary, line *CD*, is an axis of symmetry across which there are no gradients in longitudinal velocity; The top boundary and portion of the right boundary, not corresponding to the inflowing ice stream, have zero velocity (no slip, no normal flow) boundary conditions specified.

Change of ice thickness at line of symmetry

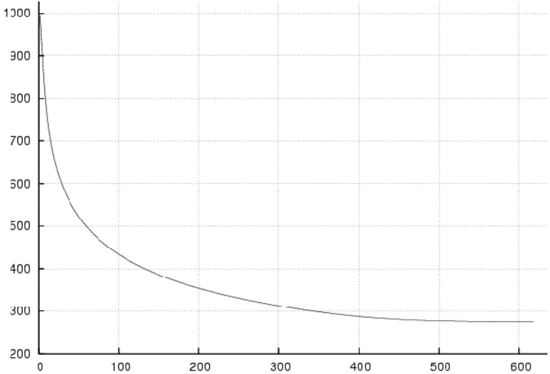

Figure: Change of ice-front thickness at line of symmetry (point *D* in Fig. 3). Equilibration is complete at about 400 years.

Contour map of ice thickness

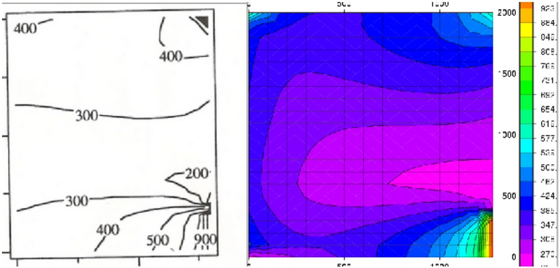

Figure: Contour map of ice thickness. Left: map generated by MacAyeal (1994). Right: map generated by our program. The ice front is on the left-hand side of the diagram; the ice-stream input is on the lower right-hand side.

Contour map of velocity magnitude

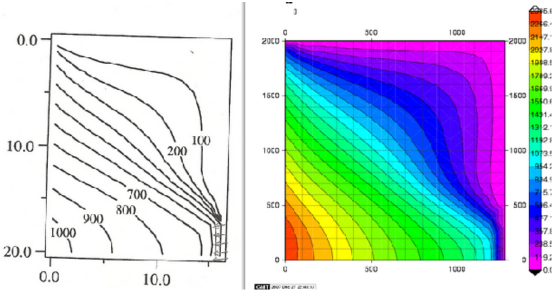

Figure: Contour map of velocity magnitude. Left: map generated by MacAyeal(1994). Right: map generated by our program. The ice front is on the left-hand side of the diagram; the ice-stream input is on the lower right-hand side.

Velocity vectors at the equilibrium

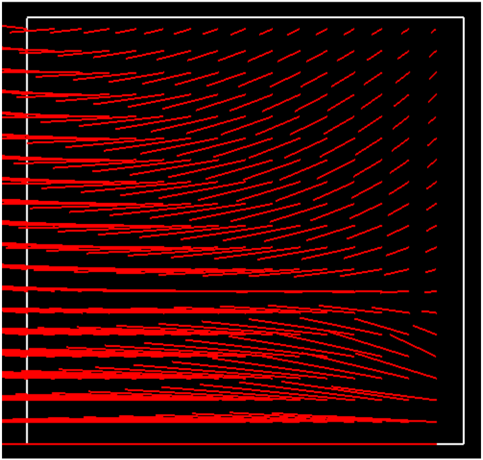

Figure: Velocity vectors after 400 years.

.

Ice thickness along the axis of symmetry

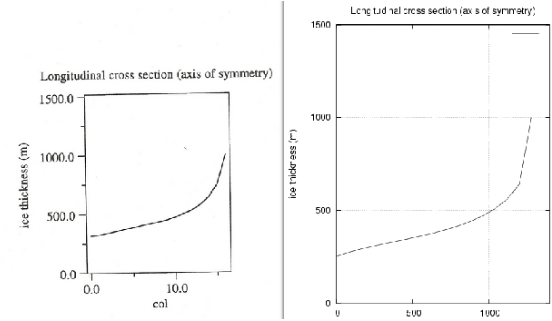

Figure: Ice thickness (m) along the axis of symmetry. Left: map generated by MacAyeal (1994). Right: map generated by our program.

Ice thickness along the transverse, midline, axis

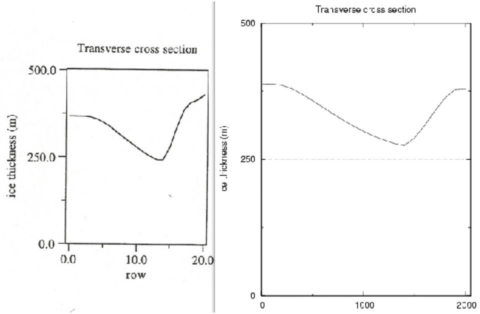

Figure: Ice thickness (m) along the transverse, midline axis of the ice shelf. Left: map generated by MacAyeal(1994) (after 150 years of evolution). Right: map generated by our program (after 400 years of evolution). Notice that the ice thickness at the stagnant side (left) of the ice shelf is slightly higher in our diagram than in the left diagram while the ice thickness in the center of the shelf (right) is slightly lower than in the left diagram. This is the result of depicting the thickness at different time of evolution.

2-D simulation of a subglacial lake

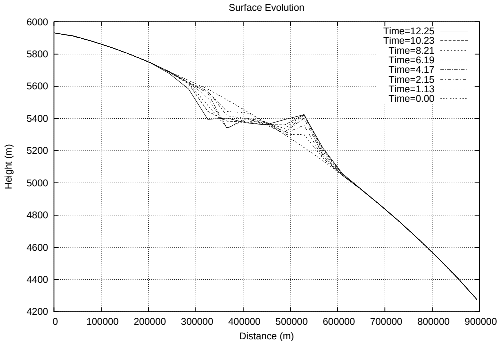

Figure: Evolution of the ice surface after invoking the stress-free boundary condition $\alpha_x = \alpha_y = 0$ at the middle of the domain; everywhere else $\alpha_x = \alpha_y = 1$. The figure demonstrates the surface flattening over a lake and creation of a rise on the down-flow edge of the lake.

2-D simulation of ice flow in a rectangular sheet-stream-shelf embayment

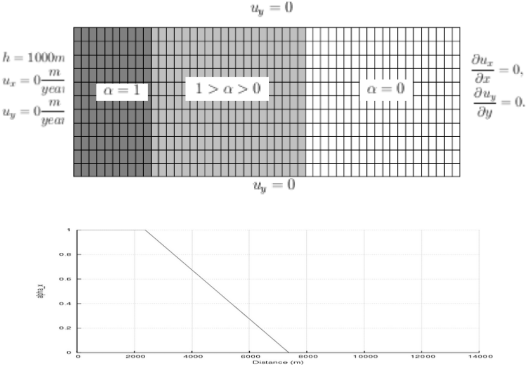

Figure: Finite Element Mesh and Parameter α_x values along the middle line of the domain. Mesh: 51x11 nodes, mesh resolution corresponds to 5 km. Ice is assumed to flow in $x-$ direction: ice sheet flow ($\alpha_x = 1$) is assumed in the $\frac{1}{5}$ of the domain, ice stream ($0 < \alpha_x < 1$) is assumed in the $\frac{2}{5}$ of the domain, and ice shelf ($\alpha_x = 0$) is assumed in the right part of the domain. Boundary conditions: the left boundary - ice-sheet; The ice front corresponds to the right boundary; The top and bottom boundary have zero $y-$ component of velocity.

Ice thickness along the middle line of the domain

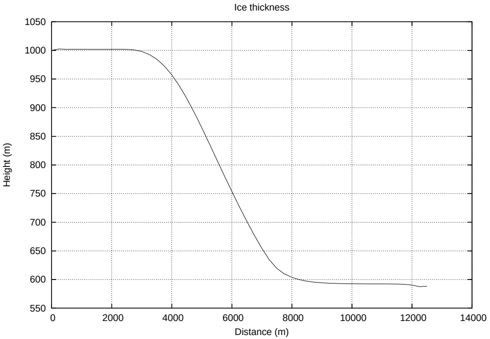

Figure: Ice thickness (m) along the middle line of the domain after imposing conditions $\alpha_x = 1$ on the left $\frac{1}{5}$ of the domain, corresponding to ice sheet, $0 < \alpha_x < 1$ on the middle $\frac{2}{5}$, corresponding to ice stream, and $\alpha_x = 0$ on the right $\frac{2}{5}$ of the domain, corresponding to ice shelf. The figure demonstrates the change of the surface curve from convex to concave over the ice stream and flattening over the ice shelf.

Table of contents

Ice stream modeling

Modified MacAyeal-Morland model

Model Verification

Summary

Summary

- MacAyeal-Morland model has been modified to include basal friction in the derivation of the equations.
- Equations allow to take into account the ice-stream bed profile.
- Basal resistive force is specified as
  - a fraction of velocity or
  - a fraction (model parameter) of the driving stress.
- In the first case, the derived equations are identical to MacAyeal-Morland equations for ice-streams.
- Simple tests have been used to verify the model.

References

- Christina L. Hulbe. *Heat Balance of West Antarctic Ice Streams, Investigated with a Numerical Model of Coupled Ice Sheet, Ice Stream, and Ice Shelf Flow*. PhD thesis, Department of Geophysical Sciences, the University of Chicago, Chicago, Illinois, 1998.
- D. R. MacAyeal. Large-scale ice flow over a viscous basal sediment: Theory and application to Ice Stream B, Antarctica. *Journal of Geophysical Research*, 94(B4): 4071-4087, 1989.
- D. R. MacAyeal. *EISMINT: Lessons in Ice-Sheet Modeling.* University of Chicago, Chicago, Illinois, 1997.
- L. W. Morland. Unconfined ice-shelf flow. in C.J. van der Veen and J. Oerlemans, editors, *Dynamics of the West Antarctic Ice Sheet*. D. Reidel, Boston, 1987
- C. R. Stokes, C. D. Clark, S. Tulaczuk. Ice stream sticky spots: A review of their identification and influence beneath contemporary and palaeo-ice streams. *Earth-Science Reviews*, 81(3-4): 217-249, 2007.

Thank You!